

# Electrical and rheological percolation behavior of multiwalled carbon nanotube-reinforced poly(phenylene sulfide) composites

B Ribeiro<sup>1</sup>, RB Pipes<sup>2</sup>, ML Costa<sup>1</sup> and EC Botelho<sup>1</sup>

Journal of Composite Materials  
2017, Vol. 51(2) 199–208  
© The Author(s) 2016  
Reprints and permissions:  
sagepub.co.uk/journalsPermissions.nav  
DOI: 10.1177/0021998316644848  
jcm.sagepub.com



## Abstract

Polyphenylene sulfide-based nanocomposites filled with unmodified multiwalled carbon nanotubes from 0.5 wt% to 8.0 wt% have been prepared by melt mixing technique with a single-screw extruder and hot press. Transmission electronic microscopy and scanning electron microscopy analysis were carried out in order to assess the multiwalled carbon nanotubes dispersion throughout the polyphenylene sulfide matrix. Electrical conductivity of the polymer was dramatically enhanced by about 11 decades between 2.0 wt% and 3.0 wt% of nanotubes, suggesting the formation of three-dimensional conductive network within the polymeric matrix. The storage modulus ( $G'$ ) of neat polyphenylene sulfide presented an increase by two orders of magnitude when 2.0 wt% of pristine multiwalled carbon nanotubes was considered, with the formation of an interconnected nanotube structure, indicative of “pseudo-solid-like” behavior. In addition, percolation networks were formed when the loading levels achieve up to 1.5 wt% for multiwalled carbon nanotubes/polyphenylene sulfide composites.

## Keywords

Polyphenylene sulfide, carbon nanotubes, electrical properties, rheological properties

## Introduction

Carbon nanotubes (CNTs) are nanoscale carbon-based materials and have received considerable attention by scientists since their first published report by Iijima.<sup>1</sup> This can be attributed to their high aspect ratio (200–1000), low density ( $\sim 2.0 \text{ g/cm}^3$ ), and remarkable electrical, thermal, and mechanical properties. Several studies involving CNTs have demonstrated that CNT can have moduli and strength levels in the range of 200–1000 GPa and 200–900 MPa, respectively.<sup>2–5</sup> These excellent properties make them useful for fabricating nanodevices and developing multifunctional composite materials.<sup>6,7</sup>

The interfacial adhesion plays an important role in composites materials. It is known that the development of CNT/polymer composites depends basically on the ability to disperse the CNTs homogeneously in the polymer matrices, i.e., the interaction between the nanofiller and polymeric matrix should be optimized. Yang et al.<sup>8</sup> reported that polymer containing aromatic ring in its structure such as polyphenylene sulfide (PPS) could have strong interaction with CNTs via  $\pi$ - $\pi$

stacking. Additionally, it was concluded that delocalization and hybridizations of  $\pi$  conduction electrons between nanotubes and polymer containing aromatic ring were common features resulting in polymer adsorption on nanotubes.

The addition of CNT into polymer matrices set a new horizon in the class of materials named electrically conductive nanostructured polymer composites. The high electrical conductivity of CNT (500–1000 S/cm) associated with their high aspect ratio allow the fabrication of materials that have gained popularity in electrostatic discharge shielding and electromagnetic

<sup>1</sup>Department of Materials and Technology, Universidade Estadual Paulista (UNESP), São Paulo, Brazil

<sup>2</sup>School of Materials Engineering, Aeronautics and Astronautics, Purdue University, West Lafayette IN, USA

### Corresponding author:

Bruno Ribeiro, Department of Materials and Technology, Universidade Estadual Paulista, Guaratinguetá, São Paulo 12516410, Brazil.  
Email: dorado.bruno@gmail.com

interference shielding applications.<sup>9–12</sup> The incorporation of CNT within a polymer is responsible for creating a CNT network, which allow a transition behavior from a semiconductive or conductive materials. This transition is a phenomenon known as electrical percolation threshold ( $\rho_c$ ), when conductive pathways are formed at a critical filler concentration in an insulating polymeric matrix. The electrical percolation threshold in CNT/polymer composites depends on the dispersion and the distribution of the nanofiller, as well as the type of the polymer and the composite processing method.<sup>13–18</sup> Additionally, the aspect ratio plays a key role during the electrical percolation threshold study. Pan and Li<sup>16</sup> studied the influence of different aspect ratio on the electrical percolation of multiwalled carbon nanotube (MWCNT)/PP composites. They revealed that as the aspect ratio becomes higher, the formation of percolated conductive network requires a lower CNT content, decreasing the values of  $\rho_c$ . In addition, according to Bangarusampath et al.,<sup>19</sup> lower percolation thresholds are associated with kinetically stabilized networks formed by nanotube agglomeration. On the other hand, higher thresholds can be associated with coating or grafting of the polymer on the CNTs, limiting intertube contacts, or with a high degree of alignment.

As an alternative to electrical characterization, dynamic rheological tests can also be employed in order to understand the formation of CNT network in composites. The dynamic and rheological studies can also predict the final properties including mechanical and electrical properties of the resultant nanostructured composites after processing. Additionally, the rheological behavior depends on the material microstructure, the state of the nanotubes dispersion, the aspect ratio and orientation of the nanotubes, the interaction between nanotubes and polymer chains, as well as nanotube–nanotube interactions.<sup>20–22</sup> It is described in literature that interconnected structures of anisometric fillers lead to deep changes in the dynamic moduli and viscosity. The storage modulus of the nanostructured composites gradually increases with increasing frequency and CNT concentration, indicating a transition from liquid-like to solid-like behavior. The CNT content at which this transition occurs is defined as the rheological percolation threshold.<sup>23–26</sup> Also, the electrical percolation threshold can be estimated by measuring the rheological counterpart because both of them reflect the formation of an MWCNT network, though these two values are different, depending on the specific composite system.<sup>16</sup>

In this study, MWCNT-reinforced PPS was prepared by melt mixing process in a twin extruder. Firstly, the morphology of composites was investigated through transmission electronic microscopy (TEM) and scanning electron microscopy (SEM) observations.

The electrical and rheological properties of MWCNT/PPS composites were investigated by the percolation threshold study. Also, it is understood that the electrical and rheological percolation thresholds can be associated to the network structure formation of MWCNT/PPS composites.

## Experimental

### Materials

PPS (Fortron 0203P6) was kindly supplied by Ticona in pellet form. This polymer presents the following physical characteristics:  $d_{25^\circ\text{C}} = 1.35 \text{ g/cm}^3$ ,  $T_g \sim 90^\circ\text{C}$ ,  $T_m \sim 280^\circ\text{C}$ . CVD pristine MWCNTs were provided by Cheap Tubes Inc. ( $d_{25^\circ\text{C}} = 2.1 \text{ g/cm}^3$ , outer diameter: 8–15 nm, inside diameter: 3–5 nm, length: 10–50  $\mu\text{m}$ ).

### Preparation of MWCNT/PPS composites

Prior to compounding, PPS pellets were ground in order to get fine powder with an average particle size of 200  $\mu\text{m}$ . In attempt to obtain a good dispersion of the nanomaterial, different concentrations of MWCNTs (0.5 wt%, 1.0 wt%, 2.0 wt%, 3.0 wt%, 4.0 wt%, 6.0 wt%, and 8.0 wt%) were physically mixed with PPS. The mixture was added in 200 ml of ethanol and sonicated in an ultrasonic bath for 30 min. Subsequently, the dispersion was partially dried in an oven at 80°C for 5 min, then sonicated for another 30 min, and heated until the ethanol was completely eliminated. A powder mixture between MWCNT and PPS has been obtained.

The melt compounding of all the mixtures was performed in a Killion KLB 100 extruder at 310°C, with a rotor speed of 70 r/min. For comparative purposes, a reference PPS was prepared in the same way.

Samples with mass of about 5 g of the extruded MWCNT/PPS were used to prepare films with a thickness around 0.5 mm. Two flat plates were used as top and bottom surfaces to guarantee uniform thickness of the thin films. In addition, a Kapton film was placed between each plate and the MWCNT/PPS mixture, in order to avoid adhesion of the material to the plates. Subsequently, homogeneous films were prepared using a Carver hot press at 310°C under 10 MPa for 1 min.

### Composite morphology

The morphology of MWCNT/PPS composites was observed using a SEM (Zeiss EVO LS-15) operating with an acceleration voltage of 15 kV. In addition, the dispersion of MWCNTs in PPS matrix was performed by transmission electron microscopy (JEOL JEM-2100) using an acceleration voltage of 200 kV. The specimen with thickness of about 70 nm was cut

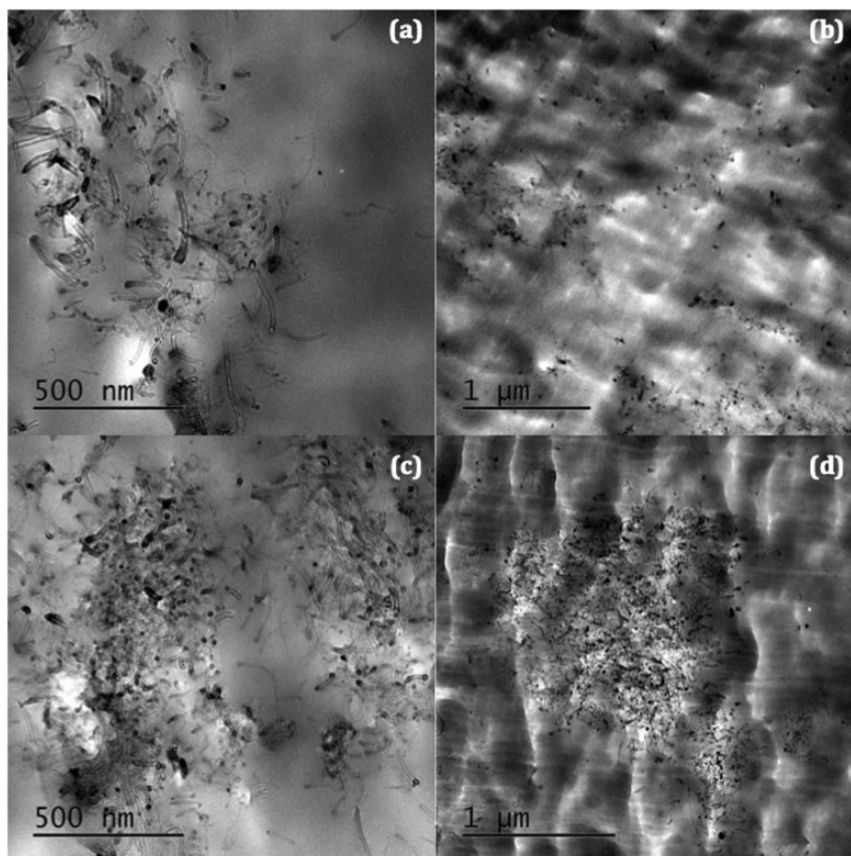


**Figure 1.** TEM images of (a and b) 1.0 wt% and (c and d) 4.0 wt% for MWCNT/PPS composites.

accordingly using an ultra microtome equipped with a diamond knife.

### Electrical conductivity

Room temperature electrical conductivity measurements were carried out on rectangular thin film samples ( $30 \times 10 \times 0.5$  mm) using a four-point probe device (Jandel Multi Height Probe) with a spacing probe  $S=0.2$  cm. A constant current  $I$  was applied to the bar specimen through two outside probes with the aid of Keithley 4200 semiconductor characterization system. The samples were freshly cleaned with ethanol prior to measurements. The tests were conducted according to ASTM D257 and the measured volume resistance,  $R_v$ , was converted to volume conductivity,  $\sigma_v$ , based on  $\sigma_v = t/R_v * A$ , where  $t$ ,  $A$ , and  $R_v$  are the thickness, area, and volume resistance of the specimen, respectively. At least five specimens for each composition were tested to report an average value.

### Rheological tests

Rheological measurements of the composites were performed using a strain-controlled rheometer (ARES of

TA Instruments) with a 25-mm diameter parallel-plate fixture. The samples about 1.0 mm in thickness were melted at  $310^\circ\text{C}$  for 5 min in the parallel plate fixture to eliminate residual thermal history and then the small amplitude oscillatory shear measurements were immediately carried out. The dynamic strain sweep measurements were first carried out to determine the linear region. Then, the dynamic frequency sweep measurements were carried out on those samples at the strain level of 1%. All measurements were performed under nitrogen atmosphere, in order to prevent oxidative degradation of the specimens.

## Results and discussions

### Morphological characterization of MWCNT/PPS composites

The evaluation of MWCNT dispersion into PPS matrix was investigated by SEM and TEM. Figure 1(a) to (d) shows typical TEM images of the composite samples with different MWCNT loadings. It can be seen that the MWCNTs have the diameter ranging from 10 nm to 30 nm and the length of several micrometers, indicating that their aspect ratio reaches values higher



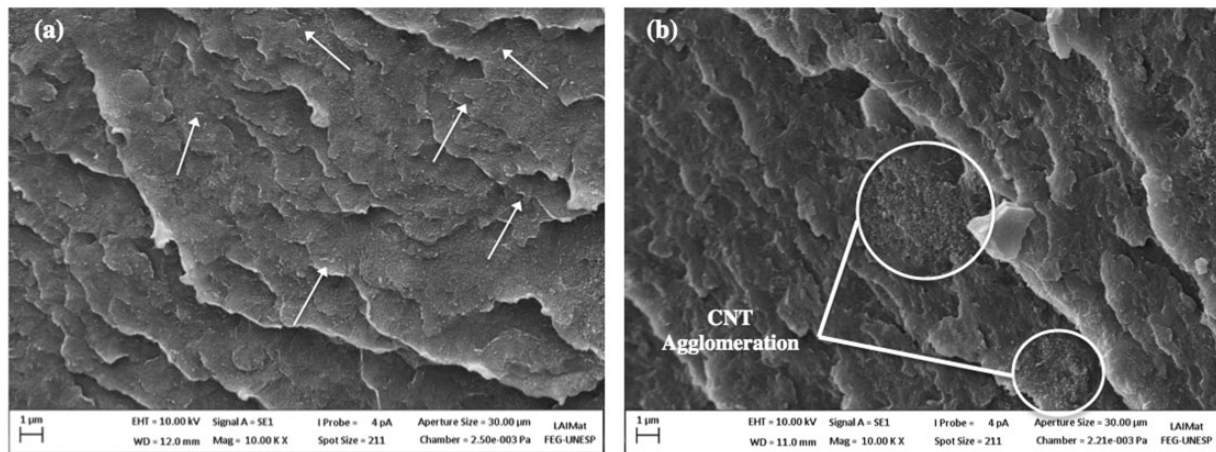


**Figure 2.** SEM images of (a) 1.0 wt% and (b) 4.0 wt% for MWCNT/PPS composites.

than 1000. Additionally, the highly curved feature of the MWCNT may be attributed to the van der Waals attractive interactions between the individual nanotubes.<sup>27</sup> It can be seen from Figure 1(a) and (b) at relatively lower loading levels (1.0 wt%), the MWCNTs are randomly and homogeneously dispersed into the PPS matrix mainly as small bundles or even individual nanotubes, presenting a good distribution. On the other hand, at high concentrations (4.0 wt%), MWCNTs are dispersed as entanglements or bundles in the polymeric matrix. In general, the MWCNTs often tend to bundle together and form some agglomeration because of the intrinsic van der Waals attractions between the individual tubes. This behavior is pointed out at high loading levels (4.0 wt%), as can be clearly seen from Figure 1(c) and (d).

In Figure 2, SEM images for the composites containing 1.0 and 4.0 wt% MWCNT are presented. The micrographs show that at 1.0 wt% loading, MWCNT are uniformly distributed in the PPS matrix. However, at high loading levels (4.0 wt%), it can be observed that the nanofillers present some agglomeration, showing some bundles. This result is in accordance to TEM images previously reported in this study.

### Electrical properties of MWCNT/PPS composites

PPS is an insulating polymer with an electrical conductivity of  $10^{-16} \text{ S cm}^{-1}$  that somewhat limits its use in the electronics and aerospace industries.<sup>28</sup> In addition, electrical conductivity higher than  $10^{-8} \text{ S cm}^{-1}$  is required for electrostatic dissipation, while for electrostatic painting and EMI shielding applications, conductivities greater than  $10^{-6}$  and  $10^{-1} \text{ S cm}^{-1}$  are required, respectively.<sup>11</sup> Figure 3 displays the electrical conductivity of PPS composites, measured at room temperature, as a

function of MWCNT concentration. It can be seen that samples with up to 2.0 wt% loading remain an insulating, showing the same behavior of neat PPS. On the other hand, for concentrations higher than that one, the electrical conductivity rises suddenly by more than 11 decades, which means that samples containing more than 2.0 wt% can be considered as electrically conductive. According to Bouchard et al.,<sup>29</sup> the electrical percolation threshold is reached when a conductive path is formed across the material from one end to the other. In addition, electrical conduction can be described by direct conduction mechanism, i.e., conductive fillers are in direct contact with each other, helping to form a conducting network within polymer matrix.<sup>20</sup> Further increasing the amount of MWCNTs beyond the percolation threshold, the electrical conductivity only increases marginally. This result can be attributed to the formation of a conducting network of MWCNTs within PPS due probably to the high aspect ratio of the filler as well as its homogeneous dispersion in polymer matrix.<sup>30</sup> It is worth to mention that at 1.0 wt%, the electrical percolation does not exist. On the other hand, samples with 4.0 wt% of MWCNTs show the region where the percolation phenomenon is already established. This information supports the concept of dispersion and homogeneity presented in morphological characterization of MWCNT/PPS composites section. Several other authors have also reported the percolation phenomenon for MWCNT-reinforced PPS composites. Yang et al.<sup>8</sup> reported a percolation threshold of 5.0 wt%, whereas Han et al.<sup>11</sup> reported a threshold of 3.0 wt%. Thus, it can be concluded that the processing conditions of MWCNT/PPS composites used in this work were satisfactory, leading to get a better dispersion of the filler into polymeric matrix and consequently, a lower electrical percolation threshold.

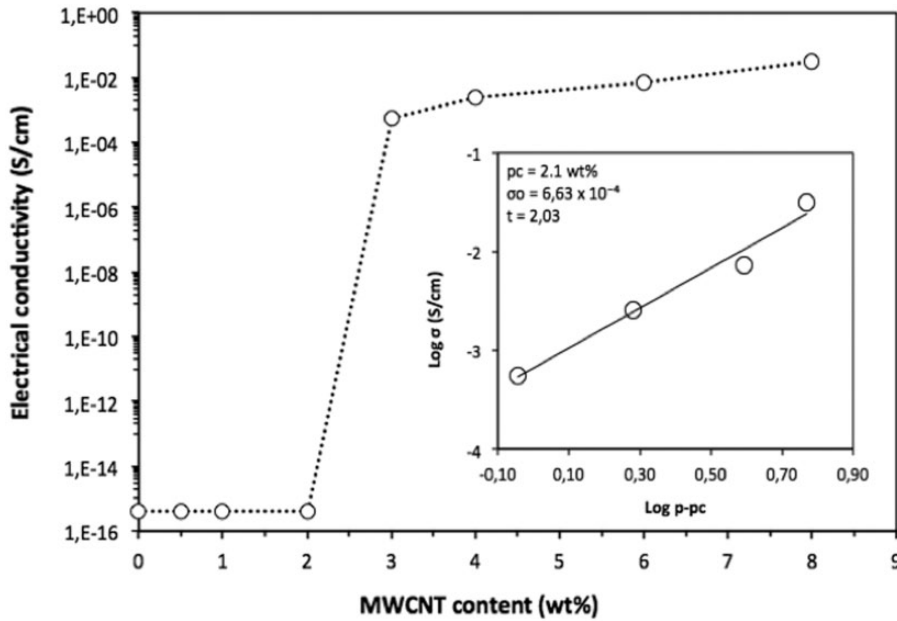


Figure 3. Electrical conductivity for MWCNT/PPS composites.

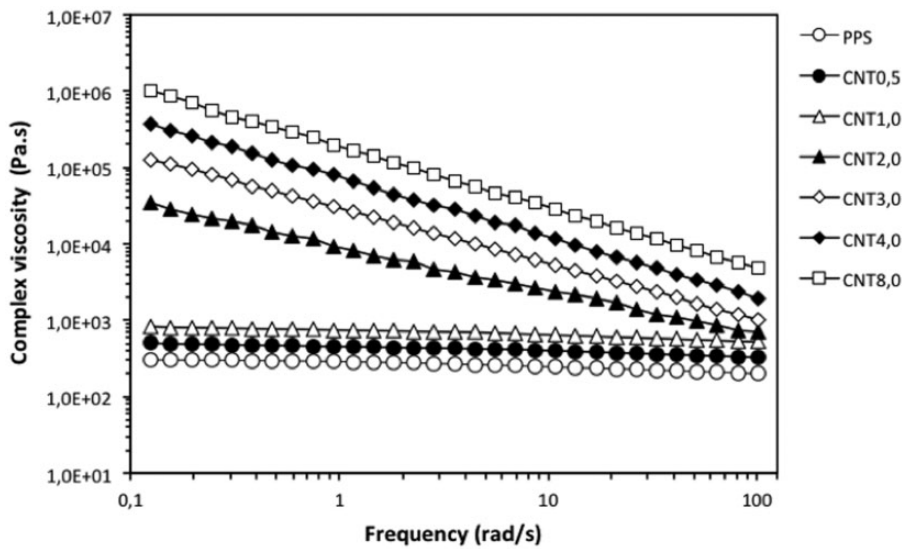


Figure 4. Complex viscosity versus frequency for MWCNT/PPS composites at 310°C.

Electrical percolation threshold ( $\rho_c$ ) can be also estimated by the classical percolation theory. A power law can be used to model conductivity of the form

$$\sigma = \sigma_0(\rho - \rho_c)^t \quad \text{for } \rho > \rho_c \quad (1)$$

where,  $\sigma$  and  $\sigma_0$  corresponds to the electrical conductivity of the composite and the conducting component, respectively,  $\rho$  is the concentration of the conducting component, and  $t$  represents critical exponent. The

values of exponent  $t$  were determined from the slope of the linear fitting on a log-log scale as seen in the inset of Figure 3.

According to the percolation theory,<sup>31</sup> the critical exponent ( $t$ ) can be defined as the average number of contacts per particle at the percolation threshold. For two-dimensional and three-dimensional systems, the values of ( $t$ ) may range from 1.1 to 1.3 and 1.6 to 2.0, respectively. However, values between 1 and 4 have been consistently reported in the literature,<sup>32-35</sup> with

no dependence on the type of polymer used, preparation method of composites, percolation threshold, CNTs features (length of the tubes, functionalization), or maximum values of electrical conductivity.

### Rheological measurements of MWCNT/PPS composites

Melt rheology can provide information about percolated network structure, dispersion state of particles, and the interaction between particles and polymer

matrix. Therefore, it is important to study the rheological behavior in order to understand the effect of the nanoparticles on internal structures and processing parameters of MWCNT/polymer composites.<sup>36,37</sup>

The complex viscosity ( $\eta^*$ ) as a function of frequency for MWCNT/PPS composites is shown in Figure 4. In general, the complex viscosity of the neat polymer is characterized by two distinct regions, called the Newtonian region and the shear-thinning region. The effect of MWCNTs on the viscosity can be pointed out at low frequencies and this behavior weakens as

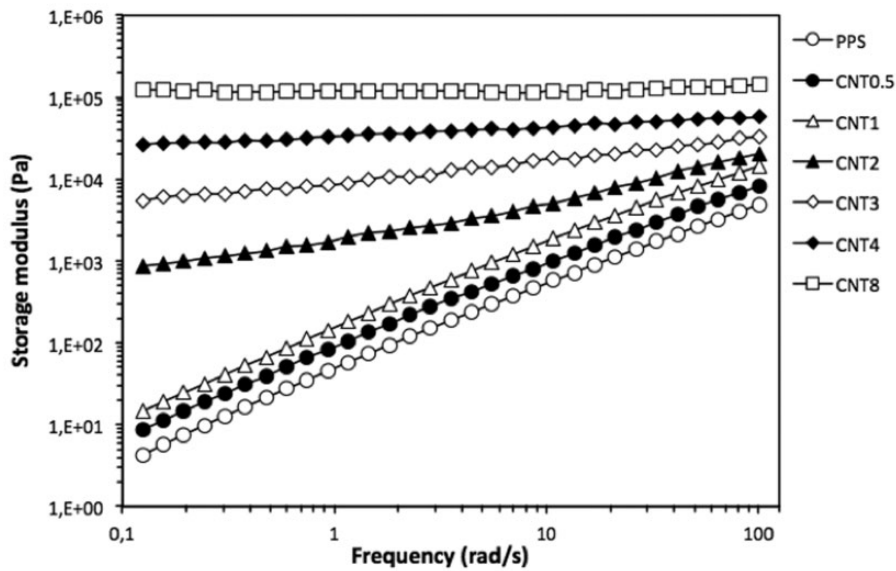


Figure 5. Storage modulus versus frequency for MWCNT/PPS composites at 310°C.

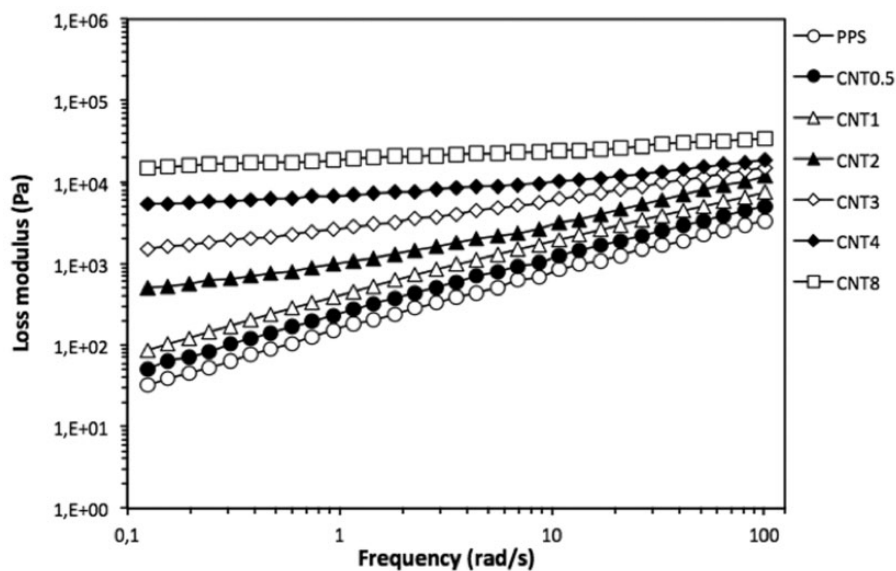


Figure 6. Loss modulus versus frequency for MWCNT/PPS composites at 310°C.

frequency increases due mainly to the shear-thinning effect. It is interesting to note that neat PPS and composites with 0.5 wt% and 1.0 wt% present a similar trend, revealing a Newtonian plateau at low frequencies, which characterizes a liquid-like behavior. However, for composites above 1.0 wt% MWCNT loading, the Newtonian region disappears and only the shear-thinning region remains at the frequency from 0.1 rad/s to 100 rad/s. Also, the viscoelastic properties are still dominated by the polymer matrix when the MWCNTs loading is low (below 1.0 wt%), and MWCNT/PPS may experience a transition from liquid-like behavior to solid-like one with MWCNTs loading up to a critical value. The critical concentration at which this transition is observed is known as the

so-called rheological percolation threshold. According to Martins et al.,<sup>38</sup> above this concentration, the tube-tube interactions play a dominant role in the rheological behavior for the composites, resulting in an increase in the complex viscosity without the Newtonian plateau region, making easy the formation of an interconnected network of CNTs within polymer matrix.

Figures 5 and 6 show, respectively, the evolution of the storage ( $G'$ ) and loss ( $G''$ ) moduli as a function of frequency for different MWCNTs contents in the PPS matrix, at 310°C. As can be seen from both figures neat PPS exhibits a typical terminal behavior, in which  $G'$  and  $G''$  followed the power laws:  $G' \sim \omega^2$  and  $G'' \sim \omega^1$ , due to full relaxation of PPS chains.<sup>39</sup> However, for concentrations above 1.0 wt% of MWCNTs, this terminal behavior disappears and the dependence of  $G'$  at low frequency is weak, which means that polymer relaxations in the composites are effectively restrained by the presence of the nanoparticles. As resulted, low frequency power-law dependence of  $G'$  decreases monotonically with increasing nanotube loading, from  $\omega^{1.73}$  for PPS to  $\omega^{0.31}$  for composite with 8.0 wt%, as listed in Table 1. These relaxation exponents are less than the expected from the theory, but this is accepted for such kind of commercial materials having large molecular weight distribution.<sup>40,41</sup> In addition, a similar trend is observed for  $G''$ . This behavior suggests that nanotube-nanotube interactions begin to dominate, eventually lead to the formation of an interconnected structure of nanotubes, which means that rheological percolation threshold is achieved.

**Table 1.** Terminal slopes of  $G'$  and  $G''$  for MWCNT/PPS composites.

System	Sample	$G'(\omega)$	$G''(\omega)$
PPS	PPS	1.73	0.83
	CNT 0.5%	1.68	0.76
	CNT 1.0%	1.65	0.75
	CNT 2.0%	0.51	0.22
MWCNT/PPS	CNT 3.0%	0.44	0.18
	CNT 4.0%	0.39	0.14
	CNT 8.0%	0.31	0.11

MWCNT: multiwalled carbon nanotubes; PPS: polyphenylene sulfide.

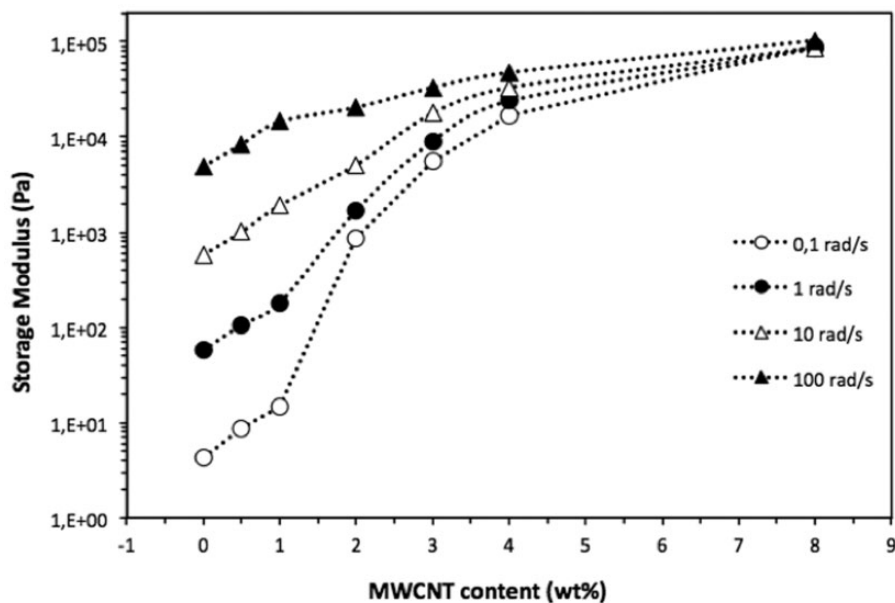


**Figure 7.** Storage modulus as function of nanotube content at different frequencies.

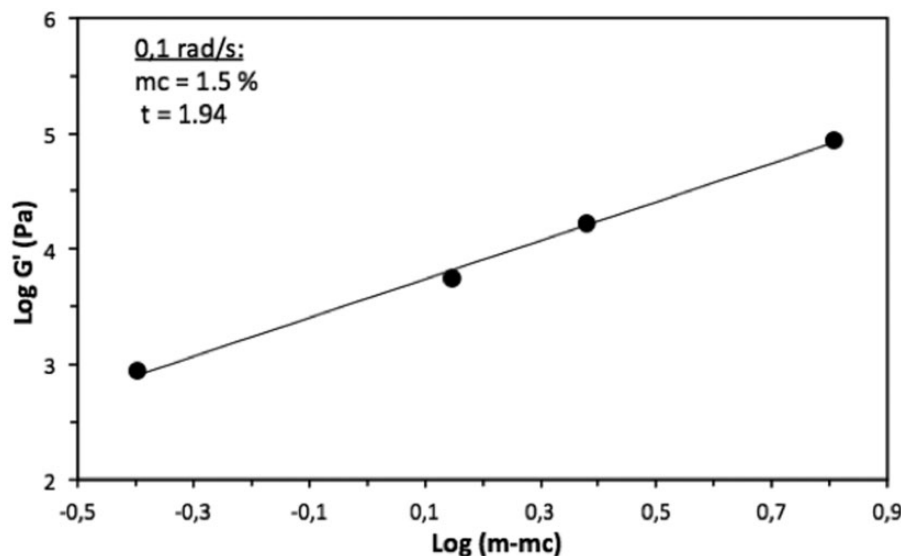


**Figure 8.** Log  $G'$  as function of Log  $m-m_c$  for MWCNT/PPS composites at 0.1 rad/s.

Figure 7 shows the storage modulus as function of nanotube content at different frequencies. As can be observed, at low frequencies, the increase in  $G'$  is not linear with composition. Also, at 0.1 rad/s and 1 rad/s, there is initially a slow rise in  $G'$  up to 1 wt% loading and between 1 wt% and 2 wt% of MWCNT, a steep slope is observed. This behavior shows the rheological percolation of the material, as previously discussed in this work. On the other hand, at high frequencies (100 rad/s),  $G'$  increases nearly linearly with the nanotube content, which means that percolation phenomenon can not be visualized at high frequencies.

Rheological percolation threshold ( $m_c$ ) can be estimated by the classical percolation theory. A power law can be used to model storage modulus of the form

$$G' \propto (m - m_c)^t \quad \text{for } m > m_c \quad (2)$$

The values of exponent  $t$  were determined from the slope of the linear fitting on a log-log scale as can be seen in Figure 8. As the MWCNTs loadings reach 8.0 wt%, the rheological parameter,  $G'$ , decreases slightly, as can be seen on Table 1. The rheological percolation threshold and the critical exponent ( $t$ ) obtained in this study for MWCNT/PPS composites were 1.5 wt% and 1.94, respectively. This suggests that a high MWCNT aspect ratio and its dispersion in PPS matrix led to a lower percolation value. Also, nanofiller network formation affected both rheological and electrical percolation obtained in this work. According to Penu et al.,<sup>20</sup> the rheological percolation threshold is reached when the CNT-CNT average distance is between the polymer entanglement distance and twice the radius of gyration, namely, from 10 nm to 100 nm. On the other hand, for electrical percolation,

the nanotubes must approach sufficiently to allow contact between particles. The rheological percolation threshold obtained was smaller than electrical percolation, supporting the theory presented in this work.

## Conclusions

Polymer nanostructured composites based on PPS and small quantities of MWCNTs were prepared by melt mixing process in an extruder, and the effects of CNTs on the electrical and rheological properties were evaluated.

The morphological observation demonstrated uniform dispersion of the MWCNT throughout the PPS matrix mainly as small bundles or even individual nanotubes at lower loading levels (1.0 wt%). However, at higher loading levels (4.0 wt%), agglomerated MWCNTs regions in PPS matrix were observed.

The electrical conductivity of MWCNT/PPS composites increased sharply around 2.1 wt% MWCNT loading, reflecting percolation behavior. The electrical percolation behavior of the polymer/MWCNT composites has been explained by the power law equation, and the correlation between the electrical conductivity and power law was in good agreement with the experimentally obtained electrical percolation thresholds.

The rheological behavior of nanostructured composites is dramatically affected by the addition of MWCNTs. Both storage and complex viscosity increase significantly after the addition of MWCNT particles at low frequencies. The rheological percolation threshold of 1.5 wt% MWCNT/PPS composites was observed. The appearance of rheological percolation can be associated with the formation of an interconnected structure of nanotubes within PPS matrix.



### Declaration of conflicting interests

The author(s) declared no potential conflicts of interest with respect to the research, authorship, and/or publication of this article.

### Funding

The author(s) disclosed receipt of the following financial support for the research, authorship, and/or publication of this article: This work was supported by CAPES (Project no. 18910-12-2).

### References

1. Iijima S. Helical microtubules of graphitic carbon. *Nature* 1991; 354: 56–58.
2. Díez-Pascual AM, Naffakh M, Marco C, et al. High-performance nanocomposites based on polyetherketones. *Prog Mater Sci* 2012; 57: 1106–1190.
3. Byrne MT and Gun'ko YK. Recent advances in research on carbon nanotube polymer composites. *Adv Mater* 2010; 22: 1672–1688.
4. Díez-Pascual AM, Guan J, Simard B, et al. Poly(phenylene sulphide) and poly(ether ether ketone) composites reinforced with single-walled carbon nanotube buckypaper: II – mechanical properties, electrical and thermal conductivity. *Compos Part A* 2012; 43: 1007–1015.
5. Ma PC, Siddiqui NA, Marom G, et al. Dispersion and functionalization of carbon nanotubes for polymer-based nanocomposites: a review. *Compos Part A* 2010; 41: 1345–1367.
6. Rahman A, Ali I, Al Zahrani SM, et al. A review of the applications of nanocarbon polymer composites. *Nano* 2011; 6: 185–203.
7. Moniruzzaman M and Winey KI. Polymer nanocomposites containing carbon nanotubes. *Macromolecules* 2006; 39: 5194–5205.
8. Yang J, Xu T, Lu A, et al. Preparation and properties of poly (p-phenylene sulfide)/multiwall carbon nanotube composites obtained by melt compounding. *Compos Sci Technol* 2009; 69: 147–153.
9. Logakis E, Pissis P, Pospiech D, et al. Low electrical percolation threshold in poly(ethylene terephthalate)/multi-walled carbon nanotube nanocomposites. *Eur Polym J* 2010; 46: 928–936.
10. Castillo FY, Socher R, Krause B, et al. Electrical, mechanical, and glass transition behavior of polycarbonate-based nanocomposites with different multi-walled carbon nanotubes. *Polymer* 2011; 52: 3835–3845.
11. Han MS, Lee YK, Lee HS, et al. Electrical, morphological and rheological properties of carbon nanotube composites with polyethylene and poly(phenylene sulfide) by melt mixing. *Chem Eng Sci* 2009; 64: 4649–4656.
12. Xin F and Lin L. Decoration of carbon nanotubes with silver nanoparticles for advanced CNT/polymer nanocomposites. *Compos Part A* 2011; 42: 961–967.
13. Chiu FY and Kao GF. Polyamide 46/multi-walled carbon nanotube nanocomposites with enhanced thermal, electrical, and mechanical properties. *Compos Part A* 2012; 43: 208–218.
14. Abbasi S, Carreau PJ and Derdouri A. Flow induced orientation of multiwalled carbon nanotubes in polycarbonate nanocomposites: rheology, conductivity and mechanical properties. *Polymer* 2010; 51: 922–935.
15. Kasaliwal GR, Pegel S, Goldel A, et al. Analysis of agglomerate dispersion mechanisms of multiwalled carbon nanotubes during melt mixing in polycarbonate. *Polymer* 2010; 51: 2708–2720.
16. Pan Y and Li L. Percolation and gel-like behavior of multiwalled carbon nanotube/polypropylene composites influenced by nanotube aspect ratio. *Polymer* 2013; 54: 1218–1226.
17. Bangarusampanth DS, Ruckdäschel H, Altstädt V, et al. Rheological and electrical percolation in melt-processed poly(ether ether ketone)/multi-wall carbon nanotube composites. *Chem Phys Lett* 2009; 482: 105–109.
18. Krause B, Boldt R, Haubler L, et al. Ultralow percolation threshold in polyamide 6.6/MWCNT composites. *Compos Sci Technol* 2015; 114: 119–125.
19. Bangarusampanth DS, Ruckdäschel H, Altstädt V, et al. Rheology and properties of melt-processed poly(ether ether ketone)/multi-wall carbon nanotube composites. *Polymer* 2009; 50: 5803–5811.
20. Penu C, Hu GH, Fernandez A, et al. Rheological and electrical percolation thresholds of carbon nanotube/polymer nanocomposites. *Polym Eng Sci* 2012; 52: 2173–2181.
21. Thomas SP, Girei SA, Atieh MA, et al. Rheological behavior of polypropylene nanocomposites at low concentration of surface modified carbon nanotubes. *Polym Eng Sci* 2012; 52: 1868–1873.
22. Zhou K, Gu SY, Zhang YH, et al. Effect of dispersion on rheological and mechanical properties of polypropylene/carbon nanotubes nanocomposites. *Eng Sci* 2012; 52: 1485–1494.
23. Zhang Q, Fang F, Zhao X, et al. Use of dynamic rheological behavior to estimate the dispersion of carbon nanotubes in carbon nanotube/polymer composites. *J Phys Chem B* 2008; 112: 12606–12611.
24. Mun SC, Kim M, Prakashan K, et al. A new approach to determine rheological percolation of carbon nanotubes in microstructured polymer matrices. *Carbon* 2014; 67: 64–71.
25. Wu D, Wu L, Zhou W, et al. Study on physical properties of multiwalled carbon nanotube/poly(phenylene sulfide) composites. *Polym Eng Sci* 2009; 49: 1727–1735.
26. Díez-Pascual AM and Naffakh M. Towards the development of poly(phenylene sulphide) based nanocomposites with enhanced mechanical, electrical and tribological properties. *Mater Chem Phys* 2012; 135: 348–357.
27. Kim JY, Han S and Kim SH. Crystallization behaviors and mechanical properties of poly(ethylene 2,6-naphthalate)/multiwall carbon nanotube nanocomposites. *Polym Eng Sci* 2007; 47: 1715–1723.
28. Noll A and Burkhart T. Morphological characterization and modeling of electrical conductivity of multi-walled carbon nanotube/poly(p-phenylene sulfide)

- nanocomposites obtained by twin-screw extrusion. *Compos Sci Technol* 2011; 71: 499–505.
29. Bouchard J, Cayla A, Devaux E, et al. Electrical and thermal conductivities of multiwalled carbon nanotubes-reinforced high performance polymer nanocomposites. *Compos Sci Technol* 2014; 86: 177–184.
  30. González-Domínguez JM, Castell P, Bispín-Gáscon S, et al. Covalent functionalization of MWCNTs with poly(p-phenylene sulphide) oligomers: a route to the efficient integration through a chemical approach. *J Mater Chem* 2012; 22: 21285–21297.
  31. Grady BP. *Carbon nanotube polymer composites: manufacture, properties, and applications*. New Jersey: John Wiley & Sons, 2011.
  32. Mamunya Y, Boudenne A, Lebovka N, et al. Electrical and thermophysical behaviour of PVC-MWCNT nanocomposites. *Compos Sci Technol* 2008; 68: 1981–1988.
  33. Chang TE, Kisliuk A, Rhodes SM, et al. Conductivity and mechanical properties of well-dispersed single-wall carbon nanotube/polystyrene composite. *Polymer* 2006; 47: 7740–7746.
  34. Yang J, Xu T, Lu A, et al. Electrical properties of poly(phenylene sulfide)/multiwalled carbon nanotube composites prepared by simple mixing and compression. *J Appl Polym Sci* 2008; 109: 720–726.
  35. Jang YK, Jang PG, Kim JK, et al. Electrical properties of imidazole-modified MWNT/polyphenylenesulfide composites prepared by melt mixing. *J Nanosci Nanotechnol* 2009; 9: 4180–4186.
  36. Botelho EC, Costa ML, Braga CI, et al. Viscoelastic behavior of multiwalled carbon nanotubes into phenolic resin. *Mater Res* 2013; 16: 713–720.
  37. Huang CL and Wang C. Rheological and conductive percolation laws for syndiotactic polystyrene composites filled with carbon nanocapsules and carbon nanotubes. *Carbon* 2011; 49: 2334–2344.
  38. Martins JN, Bassani T, Barra GMO, et al. Electrical and rheological percolation in poly(vinylidene fluoride)/multi-walled carbon nanotube nanocomposites. *Polym Int* 2011; 60: 430–435.
  39. Ferry JD. *Viscoelastic properties of polymers*, 3rd ed. New York: John Wiley & Sons, 1980.
  40. Stacy CJ. Molecular weight distribution of polyphenylene sulfide by high temperature gel permeation chromatography. *J App Polym Sci* 1986; 32: 3959–3969.
  41. Hill HW Jr. A new high molecular weight polyphenylene sulfide. *Ind Eng Chem Prod Res Dev* 1979; 18: 252–253.